16TH EUROPEAN CONFERENCE ON EARTHQUAKE ENGINEERING THESSALONIKI 18 - 21 JUNE 2018

SEISMIC NON-LINEAR BEHAVIOR OF SOIL INFERRED BY ANALYSIS OF BOREHOLE DATA

David CASTRO-CRUZ[1], Julie RÉGNIER[2], Etienne BERTRAND[3], Françoise COURBOULEX[4]

ABSTRACT

Seismic ground motion is strongly dependent on the site geotechnical characteristics. This phenomenon must be considering in risk mitigation through the evaluation of soil response. The soil response to a cyclic solicitation is not only depending on the soil parameters but also on the level of the shaking. This non-linear behavior is especially important to consider when modeling strong ground motion. We analyzed this effect using seismological data recorded in Kiban Kyoshin Network (Kik-net) localized in Japan. We use recordings from boreholes instrumented with two 3-components accelerometers, one located at surface and the other in depth. From these data, we are estimating the ground motion amplifications by computing experimental transfer functions using borehole spectral ratios (*BSR*).

The main effect of the non-linear behavior of the soil on the transfer function is a shift of the amplification towards lower frequencies and a decrease of the peak amplitudes of the soil amplification. We propose to characterize this non-linear behavior by quantifying those changes in *BSR*. This work results in site-dependent relationships between the intensity of the ground motion, expressed in terms of downhole PGA, and the modifications in the *BSR*. This article shows the used procedure for correcting surface ground motion of the soil non-linear behavior. The results obtained on several recordings of the Kumamoto earthquake show that this procedure improve the prediction of strong motion. It also highlights the usefulness of borehole seismological data to better understand and to consider the non-linear behavior of the soil.

Keywords: Nonlinearity; Borehole Spectra Ratio; Prediction of soil response

1. INTRODUCTION

It is widely recognized that this site effects can amplify dramatically the seismic motion compare to rock reference site because of seismic waves being trapped in sub-surface soft soil layers(Bard and Bouchon, 1985; Lermo and Chávez-García, 1993). The seismic site response depends on the site configuration, the nature of the soil and on the incoming ground motion. The soil behavior in the stress-strain space is nonlinear and shows hysteresis (Assimaki et al., 2008; Zeghal Mourad and Elgamal Ahmed-W., 1994). In one site, the variability of the site response is link to geometrical effects and soil behavior. For weak motion, the combination of a complex site configuration and various incident wave field can induce a variability on the site response (Thompson et al., 2009). For strongest ground motion, the soil non-linear behavior begin to have strong influence and dominate the variability on site response (Régnier et al., 2013). An accurate prediction of strong ground motion on sedimentary site will require the consideration of non-linear soil behavior.

Non-linear soil behavior is usually described by the stress-strain curves. The effects of non-linear soil

[1] PhD student, CEREMA–GeoAzur, Université Cóte d'Azur, Sophia Antipolis, France, david.castro@cerema.fr
[2] Researcher, CEREMA, Sophia Antipolis, France, julie.regnier@cerema.fr
[3] Director of Survey of Seismic Risk, CEREMA, Sophia Antipolis, France, etienne.bertrand@cerema.fr
[4] Researcher, Laboratory of GeoAzur, CNRS-UNS, Nice, France, courboulex@geoazur.unice.fr

behavior are generally a degradation of stiffness and an increase of the dissipation of energy in the material. Therefore, the stress-strain curves are approximate with the shear modulus decrease (G/Gmax) and increase of damping (ξ) curves with shear strain. In site response, the effect of non-linear soil behavior is a shift of the frequency peaks to a lower frequency bandwidth (the degradation of the shear modulus induces a decrease of the apparent shear wave velocity and consequently a decrease of the resonance frequencies of the site) and is generally associated to an attenuation of the high frequency amplification and rarely to a large increase of the high frequency (Régnier et al., 2017). This last observation has been identified as an increase of the pore water pressure when cyclic mobility occurs (Bonilla et al., 2005) or soil hardening (Pavlenko, 2017).

To estimate non-linear site response the usual practice is to use numerical simulations with equivalent linear analysis or truly non-linear time domain approach. Depending on the non-linear model, the required non-linear parameters will be different from the stress-strain curves to the shear modulus decrease (*G/Gmax*) and associated damping (*ξ*) curves with shear strain or even more advanced geotechnical parameters (Régnier et al., 2016).

The non-linear soil parameters can be characterized by laboratory tests (Ishibashi and Zhang, 1993). These methods although site specifics are associated with errors from sample disturbance, local/external measurement of the deformation and interpretation of the laboratory data (interpretation of the deformation measured with the shear strain if we are interested in shear-wave propagation). Part of these issues have been investigated but not completely solved yet (Montoya Noguera, 2016). A lower cost method is the use of non-linear parameters defined in the literature, and anchored to elastic soil properties (e.g., Darendeli, 2001; Ishibashi and Zhang, 1993). In those, using correlations between dynamic parameters and other soil parameters, likes soil classification, the modulus reduction curves are estimated.

In-situ measurements of the non-linear soil behavior are an additional method that can remove part of the errors of laboratory testing. Some authors use the accelerometer data to determine the shear-modulus reduction and damping curves. This process computes the soil non-linear parameters by finding the best soil parameters that can reproduce the accelerometers using numerical models. Other authors use interferometry between recordings at different depth to derive the instantaneous wave propagation velocity in the media depending on the input motion intensity (Bonilla et al., 2017).

Another way is to compare site-response curves computed from weak and strong motions. Some authors did visual comparison between weak and strong motion spectral ratios and found that the main differences are a shift of the frequency peaks to lower frequencies and a general decrease in the amplitude. They also mention that these differences are higher when the intensity in the incident motion increase (Aguirre and Irikura, 1997; Iai et al., 1995). Some others intend to quantify these observations. For example, (Noguchi and Sasatani, 2008), the comparison between weak and strong seismic site response is quantified by the summation of the differences between spectral ratios. They showed the link between the parameter they defined to characterize the nonlinear effects and an intensity parameter of the shaking (PGA). In (Régnier et al., 2013) several parameters are proposed to quantify those differences, and it shows that the differences are related with the intensity of the ground motion in the site.

The impact of non-linear soil behavior can be also regarded frequency by frequency using site-response curves. In (Field et al., 1997) the ratio between spectral ratios of weak and strong motions were computed with synthetic rock reference seismograms. Similarly, in (Régnier et al., 2017) the differences between the ratio of the spectral ratios are analyzed, but in this case using vertical arrays of accelerometers. Both studies indicate that the differences are frequency dependent: with the amplification being increased at some frequencies and decreased at others.

In this paper, we are following a similar approach to the previous studies that is the comparison between weak motion and strong motion site responses. Nevertheless, our objective is not to define non-linear site parameters for numerical simulations or quantification of the non-linear soil behavior, we want to

go one step further and to provide a methodology to correct the linear site response of the effects of non-linear soil behavior. We analyzed recordings from vertical arrays of Kiban Kyoshin network (KiK-Net) located in Japan. After showing the proposed methodology, an application will be performed on recordings of the 2016 Kumamoto earthquake.

2. KIK-NET DATA BASE AND SIGNAL PROCESSING

The site response can be computed with the Borehole Spectral Ratios so-called *BSR*. It is defined as the ratio between the Fourier spectrum of the seismic waves at the surface and at downhole (geometric mean of the horizontal components), the Equation (1) shows the definition of this parameter.

$$BSR(f) = \sqrt{\frac{EW_{surf} + NS_{surf}}{EW_{depth} + NS_{depth}}} \quad (1)$$

Where *BSR* represents the ratio between the ground motion at surface and at downhole. *EW* and *NS* are the discrete Fourier transform of the accelerograms for East-West, and North-south horizontal components respectively

To study the influence of the non-linear effects of the soil on the *BSR* in empirical data, the KiK-net data set in Japan was used. The KiK-net data are available in the web page of National Research Institute for Earth Science and Disaster Prevention (http://www.kyoshin.bosai.go.jp). This network is composed of 688 stations, among them, 661 have site characterizations Vs and Vp profiles, soil description and information on the stations (location and information of recording devices). For each recorded earthquake, the acceleration time histories are provided, with the event origin time, the epicenter location, the depth of the focus, and the magnitude of the earthquake determined by Japan Meteorological Agency.

Among these database, signals were selected according to two criteria: signals from earthquakes with a magnitude over 3 and with an epicentral distance shorter than 500 km. Subsequently, for all selected signal a process based on (Boore, 2005) and (Oth et al., 2011) was applied. It consists in: (1) application of automatic picking algorithm (Earle and Shearer, 1994), (2) remove the mean, (3) the previous data to the first zero-crossing point were removed, (4) The Hanning's window was applied to improve the trimming process of the signal (Oppenheim and Schafer, 2010), and finally (5) a high pass filter of 2rd order with *fc=0.*1 Hz was applied two times (Boore, 2005). This processing allows to remove unimportant effects in the data, as noisy effects, to make an easier study of the patterns and to make better comparisons. Additionally, we select just ground motions where a signal to noise ratio was upper than three in a frequency window from *0.3 Hz* to *30 Hz*.

3. EFFECTS OF THE NONLINEAR SOIL BEHAVIOUR IN THE EMPIRICAL BOREHOLE SPECTRAL RATIOS (*BSR*)

As mention in the introduction, one effect of the non-linear soil behavior is the shift of the frequency peaks in the Borehole Spectral Ratio (*BSR*) to lower range. We analyze these effects using records from Kik-Net data network to derive a methodology to correct the surface ground motion.

Using *BSR*, it is possible to study the effects of the nonlinearity similarly to previous studies (e.g., Noguchi and Sasatani, 2008; Régnier et al., 2017). In the Figure 1, four *BSR* computed from ground motions with different levels of $PGA_{downhole}$ recorded at the sale station (IBRH11) are illustrated. This figure shows that for stronger ground motions, the frequency peaks occur at a lower frequency bandwidth. This shift to lower frequencies is a direct effect of the loss of stiffness of the soil during ground shaking. We also observe a decrease in the amplitude of *BSR* which is another effect of non-linear soil behavior. It is linked to the increase of damping with shear strain in the soil.

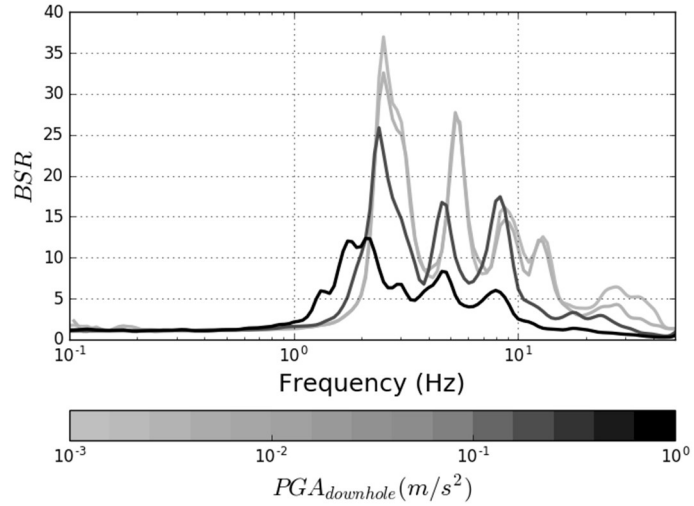

Figure 1. *BSR* for four earthquakes with different PGA at the down-hole station. This figure shows cases from the station IBRH11 from KiK-net data.

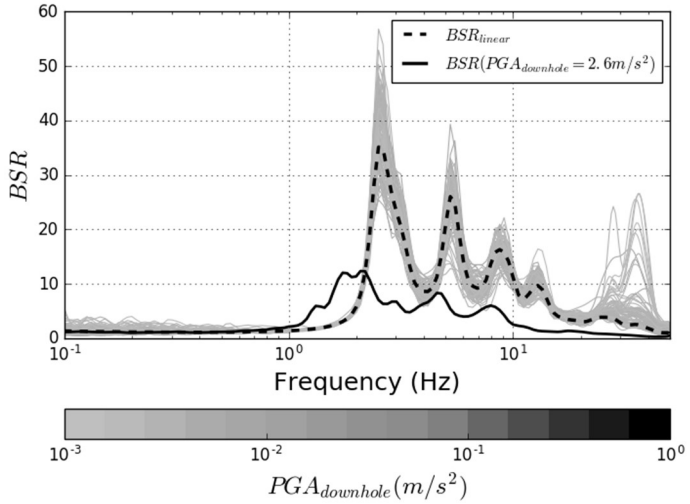

Figure 2. Definition of BSR_{linear} as the average of all the weak ground motion and comparison between BSR_{linear} with the *BSR* computed from one strong ground motion.

The Figure 1 shows that weak ground motions share a similar *BSR*. This is because for weak ground motion the soil present a linear response that makes *BSR* very similar between ground motions (Aguirre and Irikura, 1997). The variability that can be observed in the site response for weak motion is mainly linked to complex site geometry associated to various seismic waves sources (Thompson et al., 2009). To study the linear site response at each site, we define the average (geometrical) of the weak motion *BSR* that is characteristic for the linear response of the soil and called BSR_{linear}. The weak ground motions for which the soil behaves linearly were selected based on their maximal amplitude. All the ground motions with a PGA at downhole from 10^{-4} m/s^2 to $6.\ 10^{-3}$ m/s^2 were used. The Figure 2 shows the calculation of the BSR_{linear}. The dotted line is BSR_{linear}, computed from weak ground motions (the grey curves). The black line represents the *BSR* computed from a strong ground motion with $PGA_{donwhole}$ of 2.6 m/s^2. Here is easy to appreciate that *BSR*s from strong ground motions have a shift to lower frequencies and a decrease in the amplification on the peaks.

3.2 Characterization of the logarithmic frequency shift

Once BSR_{linear} is computed, this function is compared to each *BSR* from all recorded ground motions. We propose to quantify the logarithmic frequency shift to compare the curves. The logarithmic frequency shift is the gap in logarithmic scale between BSR_{linear} and *BSR*. In linear scale, it is a coefficient that changes the frequency scale. The algorithm to find this logarithmic shift minimizes the misfit

between BSR_{linear} and BSR as defined in the Equation (2). Note that the misfit is weighted by the logarithmic sampling.

$$misfit = \sum_i \left| BSR_{linear}\left(\bar{f}/_{Ls}\right) - BSR(\bar{f}) \right| \Delta x \qquad (2)$$

$$\Delta x = log_{10}(f_{i+1}/f_i) \quad and \quad \bar{f} = 0.5 \cdot (f_{i+1} + f_i)$$

The parameter *Ls* defines the shift in logarithmic scale that is applied to BSR_{linear}, that in linear scale represents a coefficient. The Equation (2) is using a discrete approximation to compute the area between BSR_{linear} and *BSR*, but with logarithmic scale as the length of the base (Δx). We selected a frequency window to evaluate the misfit that goes from *0.3 Hz* to *30 Hz* where we guarantee the records have a good signal-noise ratio (upper than 3.0).

Finally, we define a frequency shift parameter, so called *fsp,* as the square of the *Ls* that produce the minimum value of misfit. *fsp* is a coefficient that is applied to the linear resonance frequencies to obtain the non-linear ones for a specific ground motion. If no shift is needed to fit both curves, *Ls* that minimize the misfit is equal to one and then *fsp* value will be also equal to one. If BSR_{linear} is logarithmic shifted to higher frequencies to fit *BSR*, *fsp* will be higher than one. In the inverse case, if the logarithmic shift is to lower frequencies, *fsp* will be lower than one. In a linear scale, *fsp* is the square of the coefficient applied to the frequencies of BSR_{linear}. If the coefficient is lower than one, the frequencies will be lower; and the frequencies will be higher when the coefficient is higher than one.

Non-linear soil behavior is expected to logarithmic shift the site response to lower frequency range and therefore induce a *fsp* below one.

3.3 Dependency of fsp with the intensity of the ground motions

To analyze the impact of soil non-linear behavior on site response in one site, *fsp* is compared against one value that quantify the intensity of the ground motion. In the Figure 3 the *fsp* is presented against the PGA of the earthquake recorded at downhole.

The Figure 3 presents the trend between shift and intensity of the ground motion for the station IBRH11: for weak ground motion (low $PGA_{downhole}$ values), the shift is not significant and *fsp* is close to one with a dispersion that will vary from one site to another and dependent mainly on the linear site response variability. Above a threshold value of $PGA_{downhole}$, the shift due to non-linear soil behavior starts to be significant. As the peaks are shifted to lower frequencies range, the *fsp* parameter goes lower than *one* and the *fsp* curves start to decrease; this trend is similar at all stations. We proposed a non-linear fitting of the *fsp* curve as shown by the plain line in the Figure 3. We chose the hyperbolic function as it represents the *fsp* curves in most of the sites and this function (Equation (3)) is usually used to describe the modulus reduction curves (Al-Shayea et al., 2015; Coon and Evans, 1971).

$$fsp = \frac{1}{1 + \frac{PGA_{downhole}}{\theta}} \qquad (3)$$

Where θ is a parameter that describes the hyperbolic function for each site. We decided to use PGA at the down-hole ($PGA_{downhole}$) mainly because PGA is a relevant parameter for describing the amount of non-linearity a soil may produce (Régnier et al., 2013).

The Figure 4 shows the *fsp* curves for all the evaluated sites in this study. We used plain lines until the highest $PGA_{downhole}$ that has been recorded in each site, and dashed lines when the curve is extrapolated. The slope of each curve is different for each site. In some sites, the trend is quite linear meaning that there is no shift of frequency no matters the intensity of the ground motion is. In other sites, the decrease of *fsp* starts at low PGA, meaning that even for very weak motion the shift of the frequency peaks is

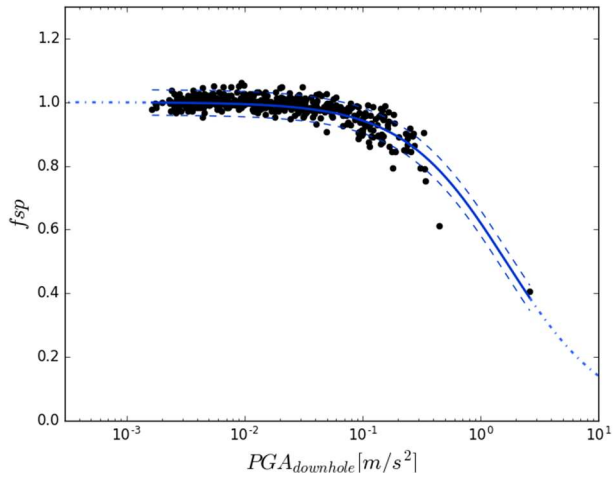

Figure 3. *fsp* value against PGA at downhole (*fsp* curves). Station IBRH11 - VS_{30}: 242.5 m/s^2

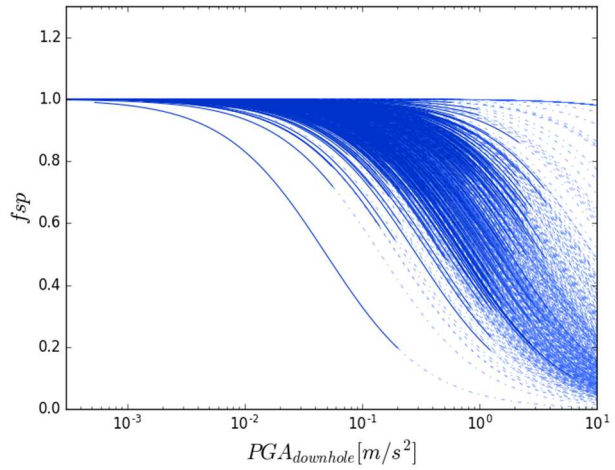

Figure 4. *Fsp* curves for all the evaluated sites from the network Kik-Net. Continue lines where the function is interpolating, dash lines when the function is extrapolating the data.

significant. The variability of the curves reflects the variability of non-linear soil behavior in all the sites. The figure shows as well, that for some $PGA_{downhole}$, all sites are prone to develop non-linear soil behavior.

3.4 Decrease of the amplification with ground motions intensity

As shown in the Figure 1 and Figure 2, the *BSR* peaks computed with weak motions have a higher amplitude than *BSR* peaks from strong ground motions. The number and the amplitude of the peaks in the *BSR* are related with the layering configuration, properties of the soils, and the depth of downhole station (Cadet et al., 2012). Based on that, we try to compare the effects of the nonlinear behavior in the amplification by comparing *BSR* against BSR_{linear} peak amplifications. We applied the previously calculated shift to be able to compare the peaks amplitude in the curves. To compare the differences between *BSR* with BSR_{linear}, we propose to use the subtraction between both curves as shown in the Equation (4):

$$\Delta BSR_{ISA}(f) = BSR(f \cdot \sqrt{fsp}) - BSR_{linear}(f) \quad (4)$$

The resulting function is called ΔBSR_{ISA} and represents the difference between *BSR* with respect to the linear soil response for each frequency. The Figure 5 shows the value of ΔBSR_{ISA} for all the ground motions in the station IBRH11. In the left plot (Figure 5A) are shown all the *BSR* for all the recorded earthquakes in this station. The right plot (Figure 5B) shows the average *BSR* for seven logarithmic equal spaced ranges of $PGA_{downhole}$. The dispersion of ΔBSR_{ISA} is large (not shown here) and the decrease of the amplification is higher for strong ground motions. Also, the peaks of ΔBSR_{ISA} are related with the

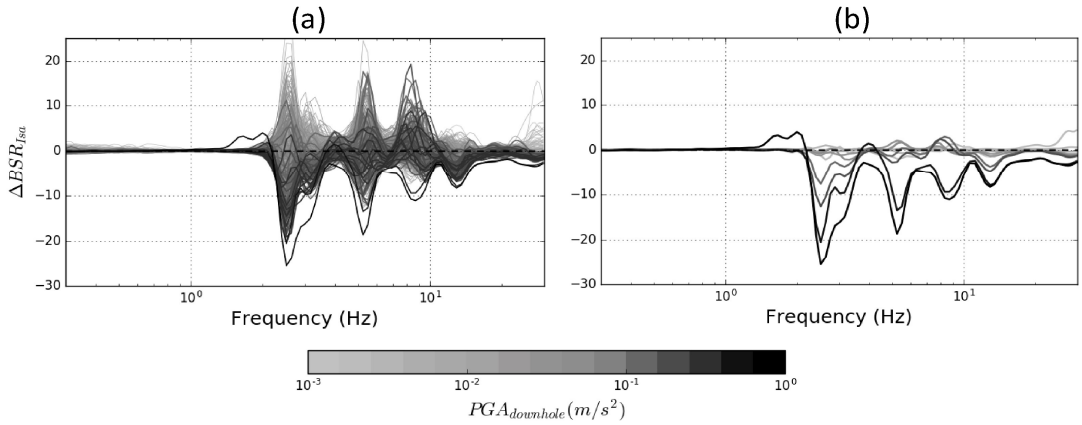

Figure 5. $\Delta BSR_{\mathrm{ISA}}$ for the station IBRH11. A) All the computed ΔBSR_{ISA} B) Average of ΔBSR_{ISA} separated by $PGA_{downhole}$ steps.

frequency peaks of $BSR_{linear.}$ Therefore, we choose to express ΔBSR_{ISA} as a function of $PGA_{downhole}$ and the BSR_{linear}.

A polynomial of grade three was chosen to fit the data through regression methodology. The variables of this polynomial are: $PGA_{downhole}$, the frequency, and BSR_{linear} (that is also in function of the frequency). For the case of the station IBRH11, the Figure 6 shows the result of the fitted surface to the data set of ΔBSR_{ISA}.

The Figure 6 shows that the decrease in the amplification is related with magnitude of $PGA_{downhole}$. This is a result of the nonlinear effects of the soil layers. The main peaks of ΔBSR_{ISA} are related with the peaks of BSR_{linear}, it means that the decrease of the amplification affects mainly the peaks. The reason could be related with an increase of the damping ratio for strong ground motion, what generates a higher impact in the peaks of the transfer function.

When the same procedure is applied to other stations, the relationships with the intensity of the ground motion and the BSR_{linear} curve remains. However, like *fsp* curves, the sensitivity to $PGA_{downhole}$ and the dispersion of the data changes.

4. METHODOLGY TO CORRECT THE NON-LINEAR SOIL BEHAVIOR

We propose a methodology to predict the non-linear surface ground motion based on the linear site response and the rock ground motion. First, the value of *fsp* for a specific earthquake, characterized by a $PGA_{downhole}$, is estimated from the non-linear regression defined in the Equation (3). With *fsp* and BSR_{linear} values it is possible to estimate the frequency peaks of the borehole spectral ratio for the analyzed ground motion. This estimation consists in applying the obtained shift (*fsp*) to BSR_{linear}. Then, the decrease in the site amplification (the surface in the Figure 6) is estimated for each frequency using BSR_{linear} and $PGA_{downhole}$. Combining the effects of the shift and the decrease of the amplification it is possible to estimate the site response of the soil for strong ground motion as shown in the Equation (5).

$$\widehat{BSR}(f) = [BSR_{linear} + \Delta BSR_{ISA}](f \cdot \sqrt{fsp}) \quad (5)$$

Where $\widehat{BSR}$, is the estimated borehole spectral ratio for strong motion, BSR_{linear} linear borehole spectral ratio, and ΔBSR_{ISA} is the estimation of the decrease of the amplification using the Equation (4), and *fsp* is the shift estimation following the fitted curved in the Equation (3).

We assume that $\widehat{BSR}$ can be used as a borehole transfer function for this specific earthquake. With this assumption, using $\widehat{BSR}$ and the ground motion at downhole it is possible to compute the ground motion at surface, as shown in the Equation (6).

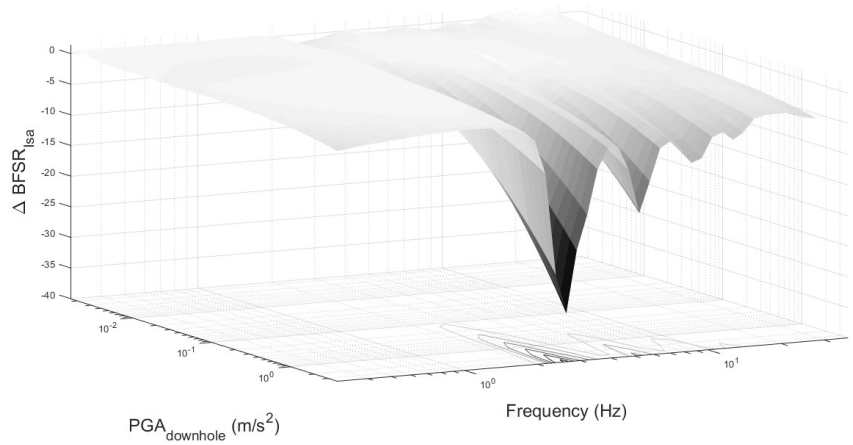

Figure 6. Fitted surface to explain ΔBSR_{ISA} from $PGA_{downhole}$, $BSR_{linear}(f)$, and frequency.

$$A_{surface} = \widehat{BSR}(f) \cdot A_{downhole} \quad (6)$$

Where $A_{surface}$ represents the discrete Fourier transform of the horizontal accelerograms at surface, $A_{downhole}$ is the discrete Fourier transform of the accelerogram at downhole, and $\widehat{BSR}$ is the estimated borehole spectral ratio computed with the Equation (5).

5. PREDICTION OF THE SURFACE GROUND MOTION OF THE 2016 KUMAMOTO EARTHQUAKE, MW 7.1

The methodology presented before is applied for the Kumamoto Earthquake occurred April 15th (UTC) of 2016 in the south of Japan (island of Kyushu), with a moment magnitude of 7.1. This earthquake is produced in the active fault, known as Futagawa fault and it was the largest earthquake in Japan for 2016 (Yagi et al., 2016). In this section, the records from this earthquake are compared with predictions using the methodology described preciously.

The methodology was applied to 2 sites of KiK-net (OITH11 and KMMH03) having recorded the Kumamoto earthquake. The Figure 7 shows the location of the two sites in the Island of Kyushu in Japan, the location of the fault and the epicenter according to (Yagi et al., 2016).

5.1 Prediction of the soil response

In the Figure 8 the *fsp* estimation is shown for OITH11 and KMMH03 sites. As it can be observed, the Kumamoto earthquake was stronger than historic records that were used to build the *fsp* curves, therefore the *fsp* estimated for this earthquake is obtained by extrapolation.

The performance of the extrapolation depends of the site and the available data. If no large or medium earthquake have been recorded at the site, the non-linear regression is not well constrained at large PGA and the estimated shift will be assorted with important uncertainties.

The estimated $\widehat{BSR}$ (using the recordings of the earthquake at downhole) at the two sites are illustrated in the Figure 9 in black thick lines along with the observed *BSR* in grey lines and the linear *BSR* in dotted line. For both cases, the application of the shift correction improves the prediction with respect to the linear soil response (BSR_{linear}). The implementation of the shift correction is important to determine in which frequencies the amplification increase or decrease in comparison with the elastic amplification. The shift in the *BSR* was well predicted even if the *fsp* was obtained by extrapolation.

In the station KMMH03 (Figure 9b) located at 27.7 km from the epicenter, the high frequency peak (around 10Hz) is not reproduce by our estimation. One possible explanation is that the station is too close to the fault that near field effects such as vertical waves is not totally accomplished in this case.

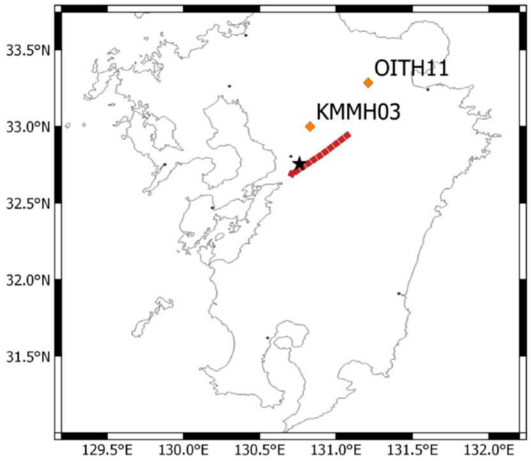

Figure 7. Island of Kiushu Japan with the location of the studied stations. The line and the star represent the location of the fault and the epicenter for Kumamoto earthquake 15th April 2016 (Yagi et al., 2016).

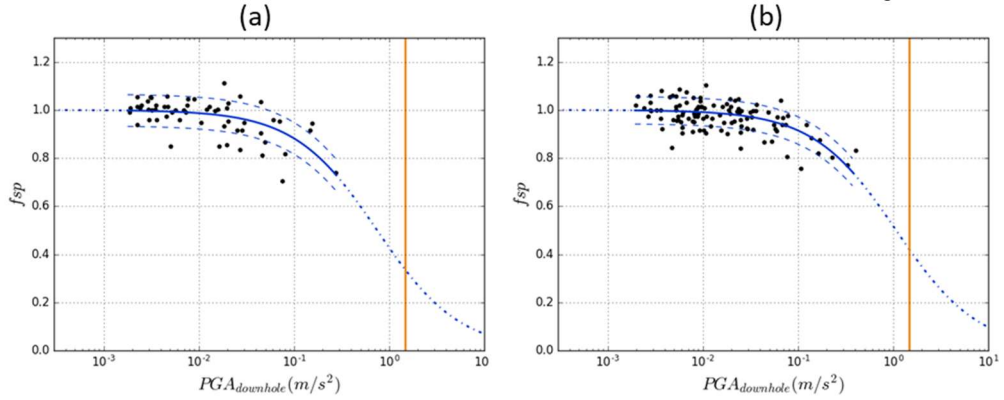

Figure 8. Evaluation of the shift to lower frequencies in function of the PGA at downhole. (a) site OITH11. (b) site KMMH03. The vertical line represents the $PGA_{downhole}$ of the Kumamoto earthquake in each station.

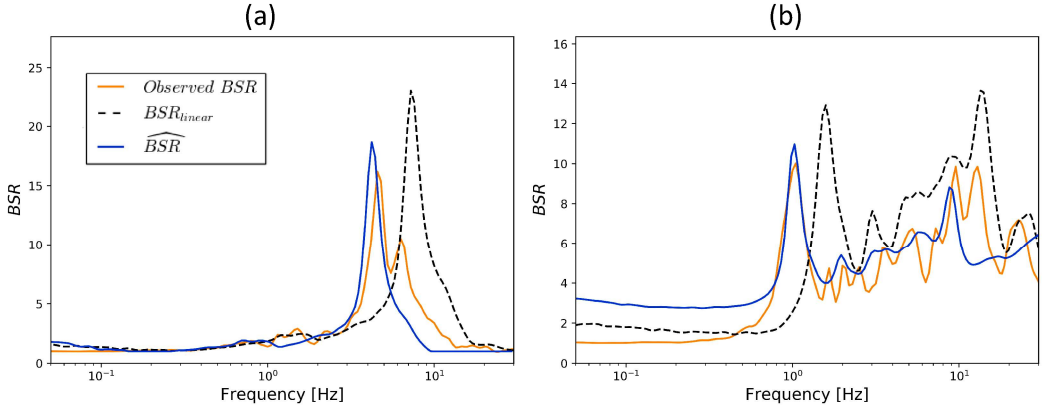

Figure 9. Comparison between the BSR_{linear} for each site (black dashed line), the observed *BSR* while the Kumamoto earthquake (gray line), and the estimation of the borehole transfer function ($\widehat{BSR}$) that is proposed (black line). (a) site OITH11. (b) site KMMH03.

This peak could be therefore linked to the source and not to the site. However, for both sites the main peaks are well predicted when the methodology proposed herein is used.

The Table 1 shows a comparison between the estimation of the main peaks with respect to the observed one in *BSR*. The differences are lower when the *BSR* is corrected by the shift and the amplitude. At both sites, the methodology improves the prediction of this frequency peak by around 50%. In the case of the amplitude, the use of the described methodology improves by more than 20% the prediction.

Table 1. Relative comparison between the main frequency peaks in the observed *BSR*, and BSR_{linear} and $\widehat{BSR}$.

	Frequency comparison		Amplification comparison	
	OITH11	**KMMH03**	**OITH11**	**KMMH03**
$BSR_{Observed}$ to $\widehat{BSR}$	8.1%	2.4%	15.8%	10.1%
$BSR_{Observed}$ to BSR_{linear}	58.3%	49.9%	42.9%	28.8%

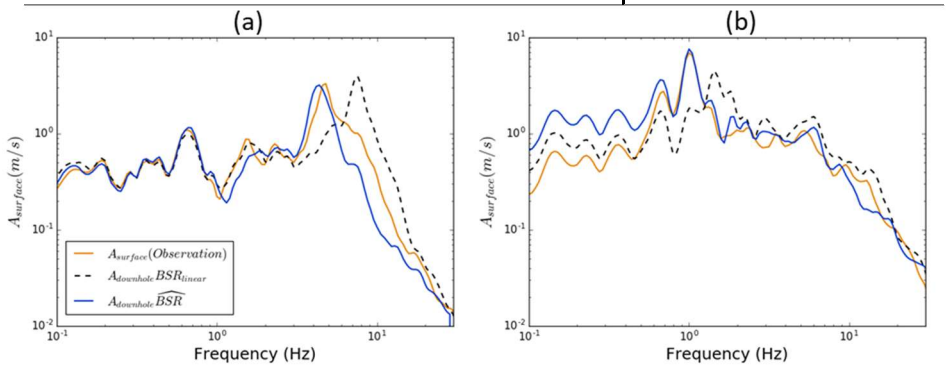

Figure 10. Fourier spectrum at surface of the horizontal components. Earthquake of Kumamoto 15th April. (a) site OITH11. (b) site KMMH03.

Table 2. Comparison of the main peaks in the spectra at surface between the observation and the computed spectra using by $\widehat{BSR}$ and BSR_{linear}.

	Frequency comparison		Amplification comparison	
	OITH11	**KMMH03**	**OITH11**	**KMMH03**
$BSR_{Observed}$ to $\widehat{BSR}$	8.8%	0.5%	1.2%	11.9%
$BSR_{Observed}$ to BSR_{linear}	58.1%	44.2%	20.6%	33.8%

As is expected from the results to predict *BSR,* the predictions of the surface ground motions are improved when the soil response (*BSR*) is corrected by the shift and the amplitude. Comparing the main peaks of the Fourier spectra at surface (Figure 10), the Table 2 shows the relative difference of the main peaks for each station. The prediction of the frequency of the main peak is improved by more than 40% in both cases, while the prediction of the maximal peak amplification is improved by 20% in comparison with BSR_{linear}.

5. CONCLUSIONS

We proposed in this paper to quantify the effects of non-linear soil behavior by the shift and the decrease of amplitude that it produces in the Borehole Spectral Ratio (*BSR)*

The logarithmic shift of *BSR*, that we called frequency shift parameter (*fsp*), is related with the intensity of the ground motion. Following this trend, we can estimate the non-linear effects for strong ground motions at sites with enough recorded data.
Similarly, we found a trend between the intensity of the ground motion and the decrease of the amplification in each frequency. The computation of this trend is still a complex process with a higher dispersion than for the *fsp* curves.

For the earthquake of Kumamoto 2016, we estimated the non-linear site response and the Fourier spectrum at surface, including the non-linear effects. The prediction provided very close results to the observations and improve by 50% the evaluation compares to a linear evaluation.

The trend of the *fsp* curves provides the propensity of a site to develop non-linearity as well a possible way to quantify the level of non-linearity of the soil under strong earthquakes.

Our work is very promising for prediction of the non-linear ground motion. However, some limitations can be mention and are the subject of current work:

- The methodology to evaluate the decrease of the amplification must be more studied and calibrated, since the selection of the surface is complex to define the trend between intensity ($PGA_{downhole}$), BSR_{linear}, frequency, and decrease of the amplification (ΔBSR).
- To estimate the ground motion at surface in time domain, the phase modification due to the site effects must be taking in account. This effect have been studied before, and usually is assumed that adding a minimal phase to spectral ratio amplitude the effect is considered (Brax et al., 2016; Fleur et al., 2016). However, since we are using borehole arrays configuration the applicability of the same assumptions must be studied.
- The methodology that we are proposing use borehole arrays, and it requires the record at the downhole station. To overpass this limitation, we can integrate this methodology directly with a numerical method to predict the rock motion at down-hole station which means that this method must estimate the effects of the down-going waves. However, this integration is a future work that should be studied continue to the work presented in this paper.
- We relate the nonlinearity of the of the soil with the intensity of the ground motion, quantified by the $PGA_{downhole}$. However, other intensity parameters could be tested in the future to reduce the dispersion of the *fsp* curves.

8. ACKNOWLEDGEMENTS

All authors are thankful with the National Research Institute for Earth Science and Disaster Resilience (NIED) in Japan for making Kik-net data available and collected the used data in this paper. Those data can be obtained from web site www.kyoshin.bosai.go.jp (last accessed October 2017).

7. REFERENCES

Aguirre, J., Irikura, K., 1997. Nonlinearity, liquefaction, and velocity variation of soft soil layers in Port Island, Kobe, during the Hyogo-ken Nanbu earthquake. Bull. Seismol. Soc. Am. 87, 1244–1258.

Al-Shayea, N., Abduljauwad, S., Bashir, R., Al-Ghamedy, H., Asi, I., 2015. Determination of parameters for a hyperbolic model of soils. Proc. Inst. Civ. Eng. - Geotech. Eng. https://doi.org/10.1680/geng.2003.156.2.105

Assimaki, D., Li, W., Steidl, J., Schmedes, J., 2008. Quantifying Nonlinearity Susceptibility via Site-Response Modeling Uncertainty at Three Sites in the Los Angeles Basin. Bull. Seismol. Soc. Am. 98, 2364–2390. https://doi.org/10.1785/0120080031

Bard, P.-Y., Bouchon, M., 1985. The two-dimensional resonance of sediment-filled valleys. Bull. Seismol. Soc. Am. 75, 519–541.

Bonilla, L.F., Archuleta, R.J., Lavallée, D., 2005. Hysteretic and Dilatant Behavior of Cohesionless Soils and Their Effects on Nonlinear Site Response: Field Data Observations and Modeling. Bull. Seismol. Soc. Am. 95, 2373–2395. https://doi.org/10.1785/0120040128

Bonilla, L.F., Guéguen, P., Lopez-Caballero, F., Mercerat, E.D., Gélis, C., 2017. Prediction of non-linear site response using downhole array data and numerical modeling: The Belleplaine (Guadeloupe) case study. Phys. Chem. Earth Parts ABC, Advance in seismic site response: usual practices and innovative methods 98, 107–118. https://doi.org/10.1016/j.pce.2017.02.017

Boore, D.M., 2005. On Pads and Filters: Processing Strong-Motion Data. Bull. Seismol. Soc. Am. 95, 745–750. https://doi.org/10.1785/0120040160

Brax, M., Causse, M., Bard, P.-Y., 2016. Ground motion prediction in Beirut: a multi-step procedure coupling empirical Green's functions, ground motion prediction equations and instrumental transfer functions. Bull. Earthq. Eng. 14, 3317–3341. https://doi.org/10.1007/s10518-016-0004-7

Cadet, H., Bard, P.-Y., Rodriguez-Marek, A., 2012. Site effect assessment using KiK-net data: Part 1. A simple correction procedure for surface/downhole spectral ratios. Bull. Earthq. Eng. 10, 421–448. https://doi.org/10.1007/s10518-011-9283-1

Coon, M.D., Evans, R.J., 1971. Recoverable Deformation Of Cohesionless Soils. J. Soil Mech. Found. Div.

Earle, P.S., Shearer, P.M., 1994. Characterization of global seismograms using an automatic-picking algorithm. Bull. Seismol. Soc. Am. 84, 366–376.

Field, E.H., Johnson, P.A., Beresnev, I.A., Zeng, Y., 1997. Nonlinear ground-motion amplification by sediments during the 1994 Northridge earthquake. Nature 390, 599–602. https://doi.org/10.1038/37586

Fleur, S.S., Bertrand, E., Courboulex, F., Lépinay, B.M. de, Deschamps, A., Hough, S., Cultrera, G., Boisson, D., Prépetit, C., 2016. Site Effects in Port-au-Prince (Haiti) from the Analysis of Spectral Ratio and Numerical Simulations. Bull. Seismol. Soc. Am. https://doi.org/10.1785/0120150238

Iai, S., Morita, T., Kameoka, T., Matsunaga, Y., Abiko, K., 1995. Response of a Dense Sand Deposit during 1993 Kushiro-Oki Earthquake. Soils Found. 35, 115–131. https://doi.org/10.3208/sandf1972.35.115

Ishibashi, I., Zhang, X., 1993. Unified dynamic shear moduli and damping ratios of sand and clay. Soils Found. 33, 182–191. https://doi.org/10.3208/sandf1972.33.182

Lermo, J., Chávez-García, F.J., 1993. Site effect evaluation using spectral ratios with only one station. Bull. Seismol. Soc. Am. 83, 1574–1594.

Montoya Noguera, S., 2016. Evaluation et réduction des risques sismiques liés à la liquéfaction : modélisation numérique de leurs effets dans l'ISS. Paris Saclay.

Noguchi, S., Sasatani, T., 2008. Quantification of degree of nonlinear site response. Presented at the 14th world conference on earthquake engineering, Beijing, Paper, p. 0049.

Oth, A., Parolai, S., Bindi, D., 2011. Spectral Analysis of K-NET and KiK-net Data in Japan, Part I: Database Compilation and Peculiarities. Bull. Seismol. Soc. Am. 101, 652–666. https://doi.org/10.1785/0120100134

Pavlenko, O.V., 2017. Possible Mechanisms for Generation of Anomalously High PGA During the 2011 Tohoku Earthquake. Pure Appl. Geophys. 174, 2909–2924. https://doi.org/10.1007/s00024-017-1558-2

Régnier, J., Bonilla, L.-F., Bard, P.-Y., Bertrand, E., Hollender, F., Kawase, H., Sicilia, D., Arduino, P., Amorosi, A., Asimaki, D., Boldini, D., Chen, L., Chiaradonna, A., DeMartin, F., Ebrille, M., Elgamal, A., Falcone, G., Foerster, E., Foti, S., Garini, E., Gazetas, G., Gélis, C., Ghofrani, A., Giannakou, A., Gingery, J.R., Glinsky, N., Harmon, J., Hashash, Y., Iai, S., Jeremić, B., Kramer, S., Kontoe, S., Kristek, J., Lanzo, G., Lernia, A. di, Lopez-Caballero, F., Marot, M., McAllister, G., Mercerat, E.D., Moczo, P., Montoya-Noguera, S., Musgrove, M., Nieto-Ferro, A., Pagliaroli, A., Pisanò, F., Richterova, A., Sajana, S., d'Avila, M.P.S., Shi, J., Silvestri, F., Taiebat, M., Tropeano, G., Verrucci, L., Watanabe, K., 2016. International Benchmark on Numerical Simulations for 1D, Nonlinear Site Response (PRENOLIN): Verification Phase Based on Canonical Cases. Bull. Seismol. Soc. Am. 106, 2112–2135. https://doi.org/10.1785/0120150284

Régnier, J., Cadet, H., Bard, P.-Y., 2017. Impact of non-linear soil behavior on site response amplitude. Presented at the Sixteenth World Conference on Earthquake Engineering.

Régnier, J., Cadet, H., Bonilla, L.F., Bertrand, E., Semblat, J.-F., 2013. Assessing Nonlinear Behavior of Soils in Seismic Site Response: Statistical Analysis on KiK-net Strong-Motion Data. Bull. Seismol. Soc. Am. 103, 1750–1770. https://doi.org/10.1785/0120120240

Thompson, E.M., Baise, L.G., Kayen, R.E., Guzina, B.B., 2009. Impediments to Predicting Site Response: Seismic Property Estimation and Modeling Simplifications. Bull. Seismol. Soc. Am. 99, 2927–2949. https://doi.org/10.1785/0120080224

Yagi, Y., Okuwaki, R., Enescu, B., Kasahara, A., Miyakawa, A., Otsubo, M., 2016. Rupture process of the 2016 Kumamoto earthquake in relation to the thermal structure around Aso volcano. Earth Planets Space 68, 118. https://doi.org/10.1186/s40623-016-0492-3

Zeghal Mourad, Elgamal Ahmed-W., 1994. Analysis of Site Liquefaction Using Earthquake Records. J. Geotech. Eng. 120, 996–1017. https://doi.org/10.1061/(ASCE)0733-9410(1994)120:6(996)